Active Sites for the Vapor Phase Beckmann Rearrangement over Mordenite: An ab Initio Study

T. Bucko,* J. Hafner, and L. Benco

Institut für Materialphysik and Center for Computational Material Science, Universität Wien, Sensengasse, A-1090 Wien, Austria

Received: July 1, 2004; In Final Form: October 15, 2004

The reaction mechanisms of the Beckmann rearrangement (BR) of cyclohexanone oxime to ϵ-caprolactam in the gas phase and catalyzed by mordenite are investigated. For the gas-phase reaction, starting with the protonated oxime, the rate-controlling step is the transformation of the N-protonated to an O-protonated species (1,2-H shift) with an activation energy of 178 kJ/mol. The barriers for the subsequent reaction steps of the transformation to N-protonated ϵ-caprolactam are significantly lower, 10 and 54 kJ/mol N-insertion and hydrolysis of the carbiminium ion. As possible active sites in the zeolite, Brønsted acid (BA) sites, silanol nests, and surface silanol groups are considered. The most favorable reaction path comprising three reaction barriers of 88, 64, and 40 kJ/mol for the 1,2-H transfer, the N-insertion, and the hydrolysis of the carbiminium ion has been found for a BA site. H-bonding is found to play a key role in the reaction catalyzed by weak acid sites. The activation energies for the rate-controlling step of the Beckmann rearrangement increases in order BA site (142 kJ/mol − 1,2-H shift + N-insertion) < silanol nest (184 kJ/mol − 1,2-H shift + N-insertion) < H-bonded terminal silanol groups (223 kJ/mol − N-insertion) < isolated silanol group (266 kJ/mol − N-insertion). We have also used harmonic transition state theory to calculate the reaction rates for catalysis by BA sites and silanol nest. Due to the large difference in the activation energies of the individual steps, the BR catalyzed by BA sites or silanol nests behave like simple first-order reactions with effective reaction barriers of 142 and 184 kJ/mol, respectively. The reaction at BA sites is about 5 orders of magnitude faster than that at a silanol nest. However, the actual turnover of a reaction catalyzed by BA sites might by slowed by the relatively high desorption energy of the product and frequent readsorption and desorption at an increased concentration of BA sites.

I. Introduction

The Beckmann rearrangement (BR) is a reaction in which oximes are transformed to the corresponding amides. The industrially important application of the Beckmann rearrangement is the conversion of cyclohexanone oxime to ϵ-caprolactam (Scheme 1). Conventionally, this reaction is carried out in sulfuric acid yielding a relatively large amount of undesired byproducts such as ammonium sulfate. Moreover, the use of fuming and corrosive sulfuric acid is problematic from an environmental viewpoint.

The environmentally acceptable alternative to the conventional process is a vapor-phase BR catalyzed by solid acids such as zeolites. Although a large research effort has been invested, the process has not been commercialized as yet. This is mainly due to problems with a short catalyst lifetime and a lower yield compared to the conventional process.[1,2] Various catalysts including zeolites (MFI,[3−8] ZSM5,[9,10] Beta,[11,12] HY,[2,12] mordenite,[12] and ferrierite[13]) have been examined. It has been found that the catalytic activity and the selectivity of the catalyst improves with increasing Si/Al ratio and that only sites with weak acidity are active in the Beckmann rearrangement.[3,4,6] Hölderich and co-workers[1,7,9,14] suggested that the catalytically active sites are silanol nests and H-bonded external silanol groups. Isolated terminal silanol groups are found to be catalytically inactive.[1,7] In contrast, Corma et al.[15,16] reported catalytic activity of strong acid sites.

SCHEME 1

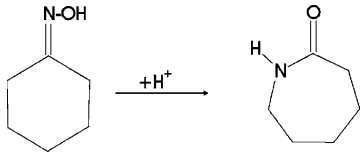

Theoretical studies of the Beckmann rearrangement have been limited to either gas-phase model assisted by strong acids such as H_2SO_4 and HCl (Nguyen et al.,[17,19,20] Fois et al.[21]) or reaction catalyzed by oxide catalysts represented by cluster models (Fois et al.,[21] Shinohara et al.,[22] Ishida et al.[23]). Recently, Yamaguchi et al.[24] and Boero et al.[25] investigated BR catalyzed by subcritical and supercritical water. In this study we use a periodic DFT ab initio technique to investigate the complete reaction mechanisms for the Beckmann rearrangement of cyclohexanone oxime to ϵ-caprolactam catalyzed by various active sites in mordenite.

II. Method

Periodic ab initio DFT calculations have been performed using the VASP code.[26−29] For the exchange-correlation functional, the generalized gradient approximation (GGA) of Perdew and Wang[30,31] has been used. The Kohn−Sham equations have been solved variationally in a plane-wave basis set using the projector-augmented-wave (PAW) method of Blöchl,[32] as adapted by Kresse and Joubert.[33] Brillouin-zone sampling was restricted to the Γ-point, the plane-wave cutoff was set to 400

* Corresponding author. E-mail: tomas.bucko@univie.ac.at

10.1021/jp0471103 CCC: $27.50
Published on Web 11/25/2004

eV. The convergence criterion for the electronic self-consistency cycle is that the change in the total energy between successive cycles must be smaller than 10^{-5} eV/atom.

Relaxation of atomic positions has been carried out in delocalized internal coordinates[34] adapted for use in periodic boundary conditions.[35−38] An improved algorithm for geometry optimization using direct inversion in the iterative subspace (GDIIS)[39] has been used. The Hesse matrix has been initialized using Lindhs model[44] and updated in the course of optimization using the Broyden-Fletcher-Goldfarb-Shanno formula (BFGS).[40−43] The ionic degrees of freedom were considered to be relaxed if all forces acting on ions were smaller than 0.05 eV/Å what typically led to convergence of the total energy to $< 2 \times 10^{-4}$ eV. The structures of transition states are identified using a drag method[45] modified for the use of internal coordinates.[37,38] The energy for a chosen degree of freedom representing the reaction coordinate is maximized, whereas all other degrees of freedom are relaxed. If the required tolerance is not reached, we use a quasi-Newton method adapted for a saddle-point search.[38] In this method we use a block Hessian in which the small block corresponding to atoms assumed to have significant components in the reaction coordinate is calculated numerically using a finite difference method, the rest of the Hessian is approximated by Lindhs model.[44] The Hesse matrix is updated using a weighted combination of Powell symmetric-Broyden (PBS)[46,47] and symmetric rank one (SR1)[48] formulas.[49] The eigenvalue spectrum of the Hesse matrix is checked upon every PBS/SR update, and only the lowest negative eigenvalue is preserved. Calculated energies for the relaxed stationary points have been corrected for zero-point vibrational energies (ZPE).

The reaction rate constants have been calculated using transition state theory[50]

$$k = \frac{k_B T}{h} \frac{Q^{\ddagger}}{Q^{\text{init}}} \exp\left(\frac{-(E^{\ddagger} - E^{\text{init}})}{k_B T}\right) \quad (1)$$

where $E^{\ddagger}$ is the energy of the saddle point, E^{init} is the energy of the reactants in the initial state, and Q^{init} and $Q^{\ddagger}$ stand for the partition functions of the initial and transition states (where the eigenfrequency corresponding to the reaction coordinate is imaginary). The analysis of the vibrational eigenstate of the complex formed by the reactants or intermediates and the active center has been performed using the force-constant approach implemented in VASP.[51,52]

The lattice parameters of mordenite have been derived from those optimized recently by Demuth et al.[53] ($a = b = 13.655$ Å, $c = 7.606$ Å). To minimize the undesired interaction between the adsorbed molecule and its replicas in the repeated cells, we used a supercell doubled in the *z* direction (i.e., $c = 15.212$). In the slab models used for representing the outer (001) surface, the lattice vector perpendicular to the surface plane was elongated in such way that the repeated layers are separated by a vacuum region of 8 Å. The lattice vectors *a* and *b* are the same as for the bulk model, $a = b = 13.655$ Å, $c = 18.500$ Å. The thickness of the slab is ∼10.5 Å.

The slab model of the (001) surface of mordenite is created from the bulk structure by cutting through the bridging oxygen atoms along a (001) plane. Equivalent surfaces are present on both sides of the slab. Under-coordinated surface O atoms have been terminated with H atoms. Out of two possible cleavage planes (see ref 54) we have chosen the one cutting through the center of the largest pores. An alternative cleavage plane would require about 50% more atoms in the unit cell. Details on the modelization of the (001) surface of mordenite can be found in our recent paper.[54] We emphasize that, although in order to limit the computational effort, the minimal slab thickness has been used in the present work, our earlier results confirm that an increased slab diameter does not lead to significant differences in the surface structure.

III. Gas-Phase Reaction

Nguyen et al.[17,19,20] proposed a simple model for the Beckmann rearrangement in which the role of the catalyst (Brønsted acid) is reduced to protonate the oxime. The reaction proceeds via the following steps: protonation of oxime → N-protonated species → 1,2-H shift → O-protonated species → migration−elimination → fragmentation products → hydrolysis → lactam. The reaction does not begin directly with the O-protonated species because of the significantly higher stability of N-protonated oxime. Using the MP2 method, Nguyen et al.[17] found that for small oxime molecules the rate-determining step is the 1,2-H shift with an activation energy >210 kJ/mol. The migration−elimination step requires an activation energy of 44 kJ/mol for the BR of formaldehyde oxime and only of 8 kJ/mol for BR of dimethyl ketoxime, respectively. The transformation of the fragmentation products into amides has not been investigated.[17,19,20]

Fois et al.[21] investigated the gas-phase mechanism for the BR of cyclohexanone oxime using the B3LYP hybrid functional.[55] The complete reaction path including hydrolysis of the fragmentation products has been determined. In agreement with Nguyen's calculations for simple oximes it has been found that the rate-determining step is the 1,2-H shift with an activation energy of 237 kJ/mol. The reaction barriers for N-insertion and for hydrolysis are 9 and 82 kJ/mol, respectively. Using the same computational method, Yamaguchi et al.[24] calculated somewhat different reaction barriers of 214, 11, and 67 kJ/mol, respectively.

The structures corresponding to stationary points on the potential energy surface for the BR of cyclohexanone oxime to ϵ-caprolactam determined in our calculations are shown in Figure 1; the corresponding reaction energy diagram is displayed in Figure 2. The N-protonated oxime R_1 is more stable by 76 kJ/mol than the O-protonated species R_2. The calculated activation energy for the rate-determining step (1,2-H shift) is 178 kJ/mol, while the reaction barriers for the N-insertion and for the hydrolysis of the carbiminium ion are 10 and 54 kJ/mol, respectively. The reaction is exothermic; the calculated heat of reaction is −176 kJ/mol. Our results agree semiquantitatively with B3LYP calculations of Yamaguchi et al.[24]

All of these data can be compared with experimental activation energies of ∼100 kJ/mol measured for several substituted oximes in different solvents.[56,57] The inconsistency between experimental and theoretical values suggests the important role of the interaction with the conjugated bases (which are, as we show later, represented by negatively charged framework in the case of zeolites) and/or with molecules of solvent.[17,18]

In the reaction mechanism discussed so far, all reaction intermediates are protonated. As we show later, if the reaction is catalyzed by weak acid sites, the reaction intermediate R_3 is already a neutral molecule, ϵ-caprolactim. The structure of this configuration is shown in Figure 3 (R_3′). Upon proton transfer from the O atom to the N atom, ϵ-caprolactam is created (P). The heat of reaction for the lactim-lactam conversion is −51 kJ/mol. The reaction barrier is 90 kJ/mol, i.e., almost doubled compared to last reaction step in the protonated model.

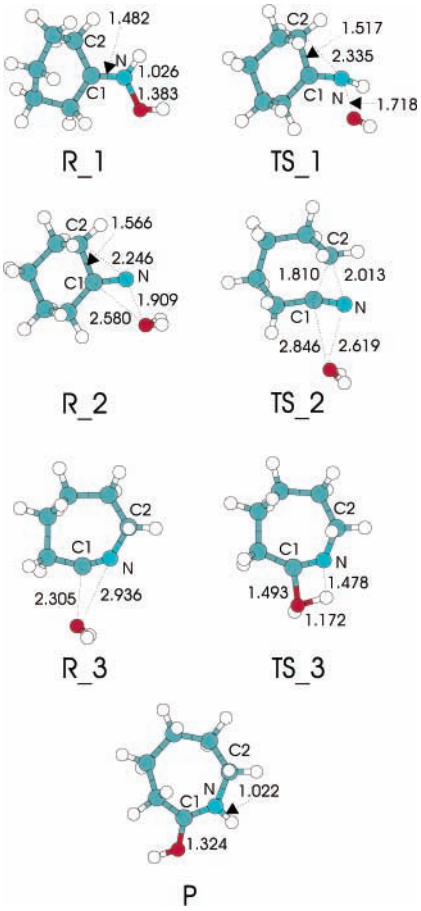

Figure 1. Structures of the reaction intermediates and product (R_1, N-protonated oxime; R_2, O-protonated species; R_3, carbiminium ion; P, N-protonated ϵ-caprolactam) and the transition states (TS_1 for 1,2-H shift, TS_2 for N-insertion, TS_3 for hydrolysis of the carbiminium ion) of the Beckmann rearrangement of cyclohexanone oxime in the gas phase. Selected bond lengths are in Å.

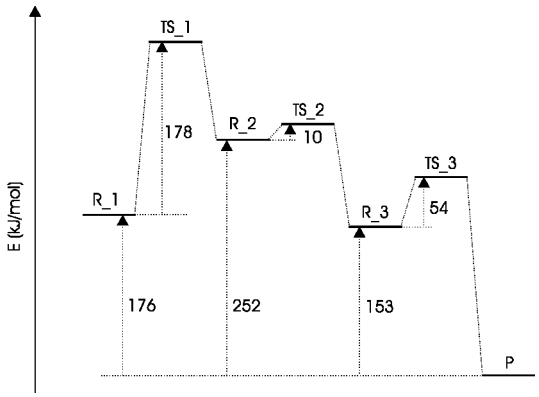

Figure 2. Reaction energy diagram for Beckmann rearrangement of cyclohexanone oxime in a gas phase. For labels see Figure 1.

This result suggests that the lactim−lactam transformation contributes significantly to the overall reaction rate. However, this is only true for the monomolecular reaction. In reality, the reaction barrier is decreased significantly if the reaction is mediated by a molecule of the solvent. As illustration we choose the reaction assisted by a molecule of water or methanol. The structures of stationary points are shown in Figure 4. We have found that the reaction barrier is decreased to only 3 and 2 kJ/mol for reactions involving water and methanol, respectively. The heat of reaction is changed less significantly, it is decreased

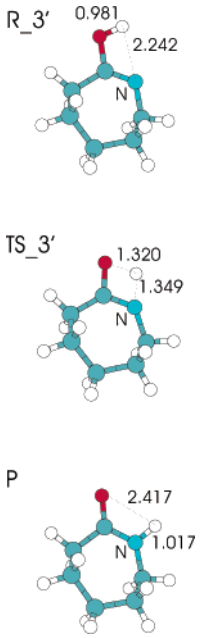

Figure 3. Gas-phase model for the transformation ϵ-caprolactim to ϵ-caprolactam: (R_3′) ϵ-caprolactim, (TS_3′) transition state, and (P) ϵ-caprolactam. Selected bond lengths are in Å.

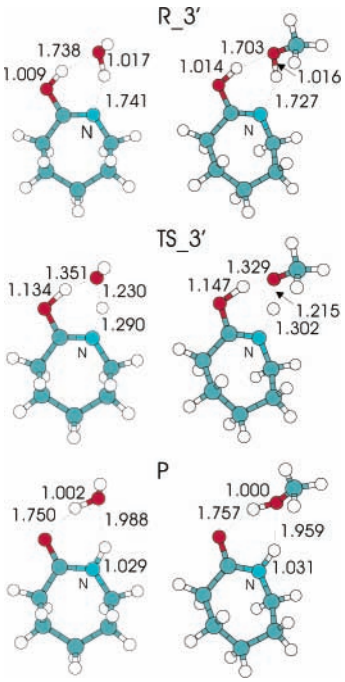

Figure 4. Lactim−lactam transformation of ϵ-caprolactam assisted by water (left) and methanol (right): (R_3′) ϵ-caprolactim, (TS_3′) transition state, and (P) ϵ-caprolactam. Interatomic separations are given in Å.

to −42 kJ/mol and −40 kJ/mol for reactions assisted by water and methanol, respectively.

IV. BR Catalyzed by Brønsted Acid Sites

A bridging OH group close to a framework Al atom represents the strongest Brønsted acid (BA) site present in zeolites. The BA site considered in this study (see Figure 5a) is located in the main channel of mordenite and is therefore accessible to bulky molecules such as cyclohexanone oxime. When interacting with the BA site via the N atom, cyclohexanone oxime forms a N-protonated species hereafter labeled R_1

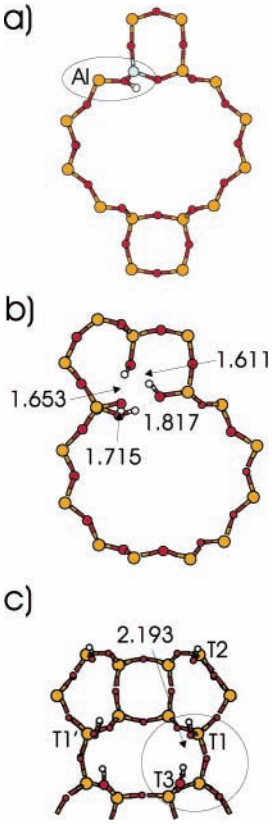

Figure 5. Brønsted acid site (a), defect with silanol nest (b), and surface silanol groups (c) considered in this study. Interatomic separations are in Å.

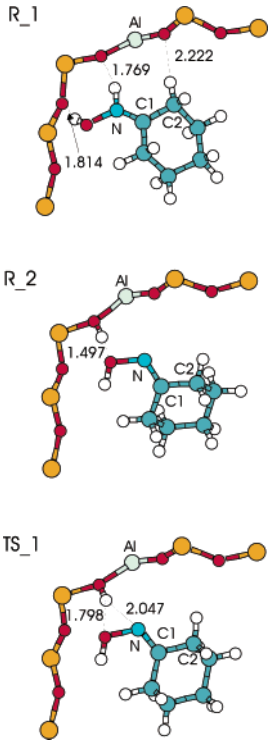

Figure 6. Adsorption complexes of cyclohexanone oxime at Brønsted acid site in the main channel of mordenite: (R_1) N-protonated complex, (R_2) H-bonded complex, and (TS_1) transition state for the transformation between R_1 and R_2. Interatomic separations are in Å.

(see Figure 6, configuration R_1). Because of a relatively strong Coulomb interaction of protonated oxime with the zeolite framework, the calculated adsorption energy is relatively large (127 kJ/mol). On the other hand, if cyclohexanone oxime interacts with the BA site via the O atom (Figure 6, configuration R_2), proton transfer does not occur and the molecule is only H-bonded to the BA site. This is an important difference compared to a gas-phase reaction in which a positive charge is carried by the oxime in all reaction steps. The calculated adsorption energy for the O-complex is 49 kJ/mol, 78 kJ/mol less than for the N-protonated complex. Hence, in analogy to the gas-phase mechanism, the reaction catalyzed by zeolite BA sites should begin from the N-protonated species.

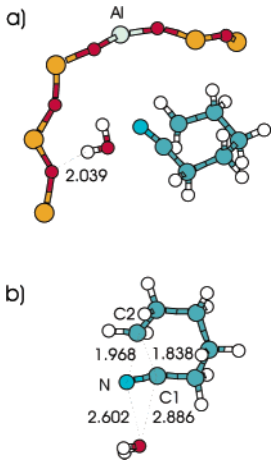

Figure 7. Transition state for the N-insertion catalyzed by Brønsted acid site in the main channel of mordenite (TS_2): (a) location of the molecule in the main channel, (b) detailed view of the transition state.

Nguyen at al. investigated the Beckmann rearrangement in sulfuric acid using ab initio techniques.[18] It was found that the presence of a solvent molecule as a co-reactant decreases the reaction barrier for the 1,2-H shift of protonated formaldehyde oxime from 234 kJ/mol[17] to 119 kJ/mol. In the presence of sulfuric acid, the 1,2 migration proceeds through a transition state in which a solvent molecule facilitates hydrogen migration between both protonated oximes by catching the migrating hydrogen from one end and putting it on the other end.[18] In the zeolite, the negatively charged framework plays the role of stabilizing basic species. The 1,2-H shift is accomplished via proton transfer from the N-protonated oxime to a framework O atom next to the Al atom, followed by the translation of oxime. The structure of the transition state is shown in Figure 6, configuration TS_1. The calculated activation energy is 88 kJ/mol, i.e., by 90 kJ/mol lower compared to the gas-phase reaction.

In the transition state for N-insertion (see Figure 7) the proton is transferred from the BA site to the OH group of cyclohexanone oxime. A water molecule is formed and detached from the rest of the molecule, the interatomic separations N−O and C1−O are 2.602 and 2.886 Å, respectively. At the same time, the C1−C2 bond is broken and the C2 atom is shifted toward the N atom such that it is located above the C1−N connection. Distances C1−C2 and N−C2 are 1.838 and 1.968 Å, respectively. Although the structure of the transition state is very similar to that for a gas-phase reaction (cf. Figure 7b and Figure 1d), the calculated activation energy of 64 kJ/mol is by 54 kJ/mol higher. The reason is the interaction with the zeolite framework which stabilizes the reaction intermediates even more than the transition state. Similar effect has been observed by Yamaguchi et al.[24] who found that the activation energy for the N-insertion increases by ∼50 kJ/mol if the gas-phase reaction is assisted by a water molecule.

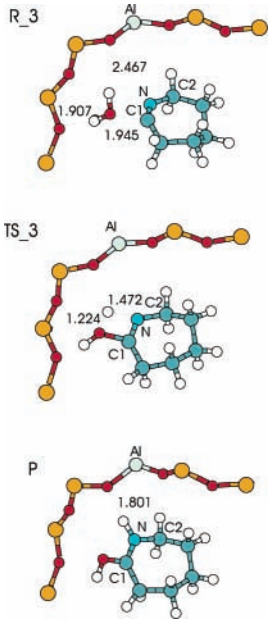

Figure 8. Hydrolysis of the carbiminium ion in the main channel of mordenite: (R_3) carbiminium ion and water molecule, (TS_3) transition state, and (P) reaction product (N-protonated ϵ-caprolactam). Interatomic separations are in Å.

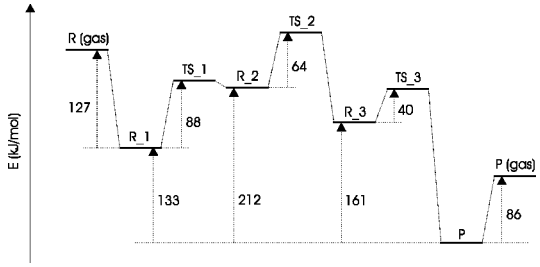

Figure 9. Reaction energy diagram for Beckmann rearrangement catalyzed by Brønsted acid site in mordenite. Labels are as in Figures 6−8.

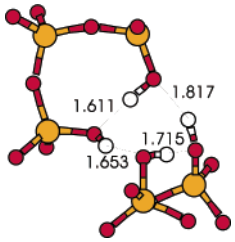

Figure 10. Detailed view of the defect with silanol nest. Lengths of H-bonds are in Å.

As a reaction intermediate (R_3) a carbiminium ion is formed. The structure of configuration R_3 is shown in Figure 8. At this point, the N atom is incorporated in the C_6N ring. The water molecule is still separated from the carbiminium ion, but the O−C1 distance is shortened to 1.945 Å. Compared to configuration R_2, this complex is more stable by 51 kJ/mol. This is significantly less than the energy difference between the R_2 and R_3 configurations in the gas-phase reaction ($\Delta E = 99$ kJ/mol).

The final step of the reaction is the hydrolysis of the carbiminium ion. The water molecule approaches the carbiminium ion and the length of one of the OH bonds increases. In the transition state TS_3 (displayed in the middle panel of Figure 8), an H atom from the water molecule is located between the O and N atoms, the separations O−H and N−H are 1.224 and 1.472 Å, respectively. The activation energy for this part of the reaction is 40 kJ/mol, i.e., only by 14 kJ/mol lower compared to that for the gas-phase reaction.

Upon hydrolysis of the carbiminium ion, O-protonated ϵ-caprolactam is formed (see Figure 8, configuration P). The adsorption energy of ϵ-caprolactam in mordenite is 86 kJ/mol. This high value indicates that the desorption of the reaction product from the zeolite might contribute significantly to the overall reaction rate. The calculated heat of reaction for hydrolysis is −161 kJ/mol, i.e., almost the same as that for the gas-phase model. The potential energy diagram for all steps of the reaction is shown in Figure 9.

Our results can be compared with semiempirical MNDO calculations of Shinohara et al.[22] They found activation energies of ∼20 and 372 kJ/mol for 1,2-H shift and for N-insertion, respectively. The BA site was represented only by a minimal cluster; the interaction with the zeolite framework, which, as we have shown, is very important, was therefore completely neglected. It should be also noted that low-level theory methods such as MNDO can provide only very rough description of complicated chemical systems such as zeolites.

To summarize, catalysis of the BR of cyclohexanone oxime by a BA site in a zeolite leads to significant changes in the reaction profile compared to the gas-phase reaction. Although the 1,2-H shift is still the step with the highest reaction barrier, the corresponding activation energy is decreased from ∼178 kJ/mol to ∼88 kJ/mol. On the other hand, due to a weaker stabilization of the transition structure by the zeolite framework compared to the reaction intermediates, the activation energy for the N-insertion is increased from ∼10 kJ/mol to ∼64 kJ/mol. As the reaction intermediates and transition state for the hydrolysis of the carbiminium ion are stabilized by interaction with zeolite framework by about the same amount, the energy profile for hydrolysis is very similar to that calculated for the gas-phase reaction.

V. BR Catalyzed by Silanol Nests

A silanol nest is a structural defect formed upon removing a tetrahedral site from the framework and termination of the dangling bonds of four O atoms by H atoms. The structure of the silanol nest considered in this study is shown in Figure 5b, a detailed view is shown in Figure 10. Every silanol group in the silanol nest is H-bonded to the O atom of neighboring OH group; the lengths of H-bonds vary between 1.611 and 1.817 Å.

The most stable adsorption complex found for cyclohexanone oxime at a silanol nest is shown in Figure 11 (R_1). In analogy to the complex R_1 formed at a BA site, this configuration is N-protonated. Interestingly, the OH bonds in the silanol nest are rearranged in such way that a siloxy group is formed in a position in which it can be stabilized by two strong H-bonds of lengths of 1.299 and 1.410 Å. In addition, the OH group of the oxime is H-bonded to one OH group of the silanol nest. The length of this contact is 1.498 Å. The calculated adsorption energy is 56 kJ/mol, i.e., by 71 kJ/mol lower compared to adsorption at a BA site. This result indicates that if both BA sites and silanol nests are present in the zeolite, cyclohexanone oxime should be preferentially adsorbed at BA sites.

An adsorption complex in which the OH group of the oxime interacts with both O and H atoms of the silanol nest is shown in Figure 11 (R_2). In this complex the cyclohexanone oxime molecule remains neutral. The O-interacting configuration R_2 is less stable than the N-protonated structure R_1; the difference in total energies is 35 kJ/mol. As in the case of BR catalyzed

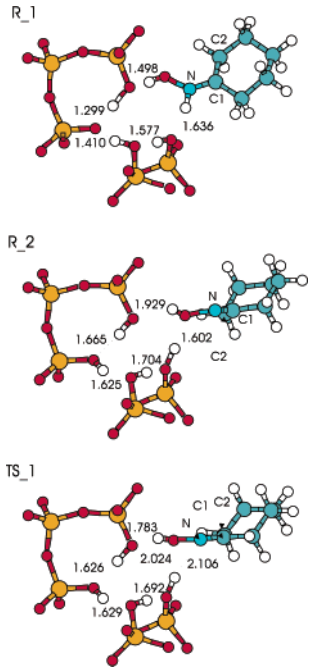

Figure 11. Adsorption complexes of cyclohexanone oxime at defect with silanol nest in mordenite: (R_1) N-protonated complex, (R_2) H-bonded complex, and (TS_1) transition state for the transformation between R_1 and R_2. Interatomic separations are in Å.

by a BA site, the reaction should begin from the N-protonated complex R_1, which is transformed into the H-bonded complex R_2 in the first reaction step.

The structure of the transition state is shown in Figure 11 (TS_1). At this point, the proton is transferred from the N atom of the oxime to the nearest OH group of the silanol nest, distances H−N and H−O are 2.106 and 2.024 Å, respectively. Again, this process is followed by a rearrangement of the OH groups of the defect (cf. Figure 11 (TS_1,R_1) and Figure 10). The calculated activation energy for this step is 42 kJ/mol. This value is significantly lower compared to that for a BR catalyzed by a BA site (see section IV).

In analogy to the reaction at a BA site, N-insertion is accompanied by the formation of a water molecule from the OH group of the oxime and a H atom of the H-bonded silanol group. As in the case of configuration R_1, the siloxy group is not formed in the place of the H donating silanol group. The system of H-bonds in the silanol nest allows H atoms to migrate from one Si−O group to another. In the transition state shown in Figure 12, a siloxy group is created in the position in which it is stabilized by two strong H-bonds of lengths of 1.349 and 1.505 Å. The structure of the oxime in the transition state is remarkably similar to that for a gas-phase reaction and for the reaction catalyzed by a BA site (cf. Figure 1 (TS_1), Figure 7b, and Figure 12b). Despite this obvious structural similarity, the calculated activation energy for N-insertion at a silanol nest of 149 kJ/mol is the highest among the models discussed so far. The creation of an energetically disadvantageous siloxy group is therefore only partially stabilized by H-bonds.

Upon N-insertion, the proton is transferred back to the silanol nest and the original arrangement of silanol groups in the nest is restored. In this process a neutral molecule of ϵ-caprolactim is formed (see Figure 13 (R_3)). This is an important difference compared to the reaction catalyzed by a BA site in which the configuration R_3 contains a carbiminium ion and a water molecule (see Figure 8 (R_3)).

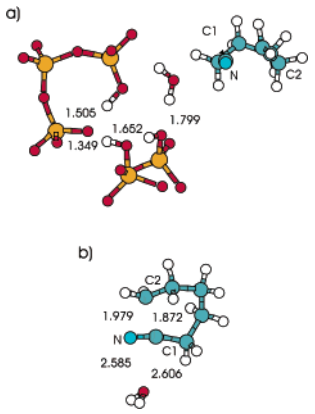

Figure 12. Transition state for the N-insertion catalyzed by silanol nest in mordenite (TS_2): (a) position of molecules with respect to silanol nest, (b) detailed view of the transition state.

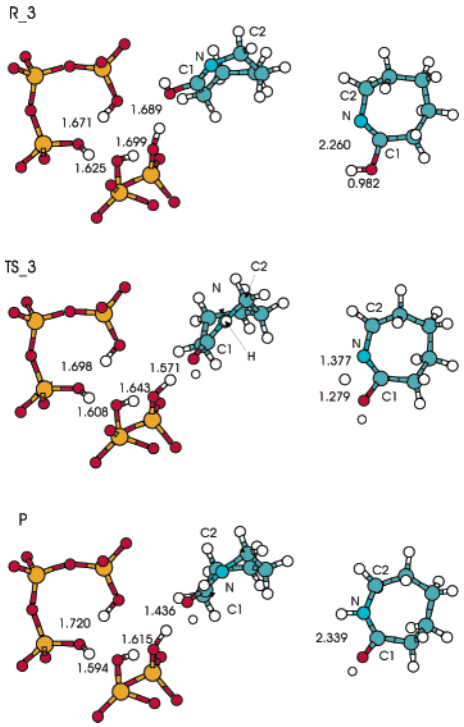

Figure 13. Lactim−lactam transformation of ϵ-caprolactam at silanol nest: (R_3) ϵ-caprolactim, (TS_3) transition state, and (P) ϵ-caprolactam. Interatomic separations are in Å.

The last reaction step is a lactim−lactam transformation, i.e., the migration of the H atom from the OH group to the N atom of ϵ-caprolactam. The reaction intermediates (R_3, P) and the transition state (TS_3) for this transformation are shown in Figure 13. The calculated activation energy of 72 kJ/mol is lower than that for a gas-phase reaction. As shown in section III, this reaction barrier is significantly decreased if solvent molecules take part in the reaction. The adsorption energy of ϵ-caprolactam in the final configuration is 28 kJ/mol. Desorption of the ϵ-caprolactam from a silanol nest should be thus easier than desorption from a BA site. Altogether the reaction energy profile for the reaction catalyzed by a silanol nest (see Figure 14) differs significantly from a gas-phase reaction and from a BR catalyzed by a BA site.

VI. BR Catalyzed by Terminal Silanol Groups

As a model for terminal silanol groups at the (001) surface of mordenite, we have chosen the H-bonded silanol pair T1

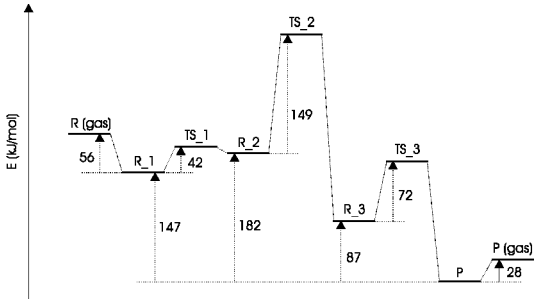

Figure 14. Reaction energy diagram for Beckmann rearrangement at silanol nest in mordenite. For labels see Figures 11−13.

and T3 (see Figure 5c). The length of the H-bond is 2.193 Å. In all models discussed so far the reaction begins with N-protonated oxime which is significantly more stable than the neutral O-interacting species. Terminal silanol groups are, however, less acidic than BA sites, and if they are not involved in a silanol nest they cannot protonize cyclohexanone oxime. We have identified two adsorption complexes in which cyclohexanone oxime interacts with a terminal silanol group via the N atom. In the configuration displayed in Figure 15a, both N and O atoms of cyclohexanone oxime are acceptors of H-bonds with terminal silanol groups; the corresponding lengths are 1.644 and 1.881 Å, respectively. The calculated adsorption energy for this configuration is 76 kJ/mol. In the second adsorption complex (see Figure 15b), oxime interacts with the silanol groups in such a way that the N atom is acceptor and the O atom is a donor of H-bond, the lengths of H-bonds are 1.708 and 1.895 Å, respectively. This adsorption complex is only slightly less stable than the previous one, the calculated adsorption energy is 74 kJ/mol. A configuration in which the oxime interacts with terminal silanol groups solely via its OH group is shown in Figure 15c. The OH group of the oxime connects the silanol groups T1 and T2 in such a way that a chain of four H-bonded OH groups is formed, the lengths of the corresponding H-bonds vary between 1.700 and 1.915 Å. The adsorption energy for this configuration is 77 kJ/mol, i.e., only slightly higher than the adsorption energy for the most stable configuration with the H-bonded N atom. As the differences in the adsorption energies are only very small, all types of adsorption complexes are expected to be about equally populated. In our analysis of the reaction mechanism we start with the adsorption complex interacting with silanol groups only via its OH group, which is analogous to the configurations R_2 in silanol nest and BA sites.

As in all models discussed in this study, N-insertion is accompanied by the formation of a water molecule from the OH group of cyclohexanone oxime and a H atom from the silanol group T1. As in the case of the reaction at a silanol nest, an energetically disadvantageous siloxy group is formed. However, its stabilization is much less efficient than in a silanol nest. This is because the chain-like organization of H-bonded OH groups does not allow such rearrangement of the positions of the H atoms as in a silanol nest. Thus the siloxy group is created directly at the place of the proton-donating silanol group T1. The structure of the transition state is shown in Figure 16. The water molecule is H-bonded to O atoms of the siloxy group and of the silanol group T2, the lengths of the H-bonds are 1.643 and 2.069 Å, respectively. The H-bond between the siloxy group and the H atom of the silanol group T3 is strengthened, as indicated by its shortening from 1.915 Å in the reactant configuration (Figure 15 (R_1)) to 1.514 Å in the transition state (Figure 16). As a consequence of the insufficient stabilization of the siloxy group in the transition state, the reaction barrier

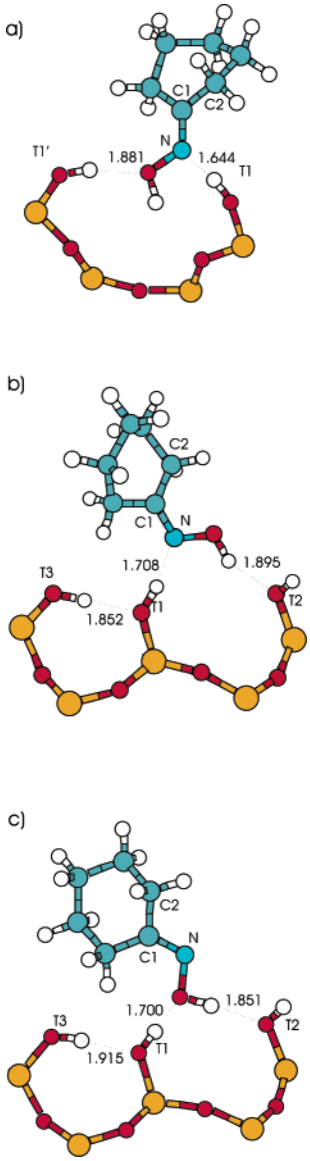

Figure 15. Three adsorption complexes of cyclohexanone oxime at surface silanol groups, cf. text. Lengths of H-bonds are in Å. The calculated heats of adsorption are 80 kJ/mol (a), 74 kJ/mol (b), and 82 kJ/mol (c), respectively.

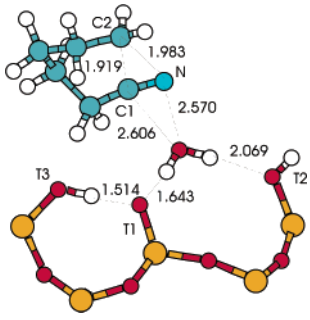

Figure 16. Transition state for the N-insertion catalyzed by H-bonded silanol groups at external surface of mordenite (TS_2). Selected interatomic distances are in Å.

is dramatically increased compared to a reaction at a silanol nest, the calculated activation energy is 223 kJ/mol. This means that the energy of the transition state is substantially higher than the desorption energy of the reactant.

The reaction intermediate created upon N-insertion is a lactim tautomer of ϵ-caprolactam (see in Figure 17 (R_3)). Similarly,

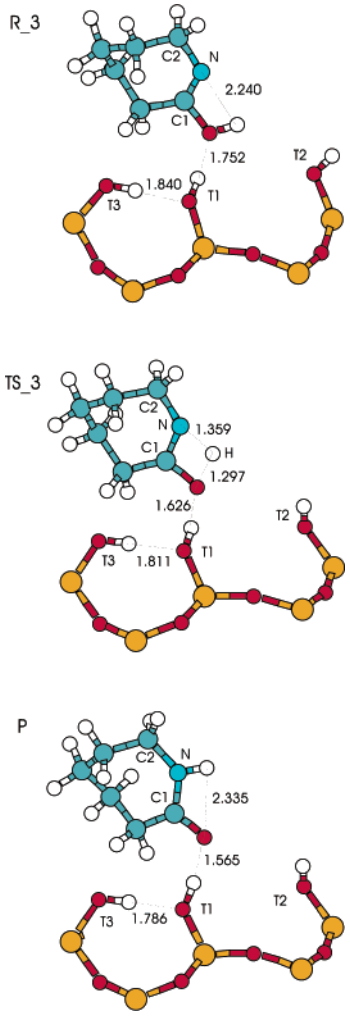

Figure 17. Lactim−lactam transformation of ϵ-caprolactam at H-bonded surface silanol groups: (R_3) ϵ-caprolactim, (TS_3) transition state, and (P) reaction product. Interatomic separations are in Å.

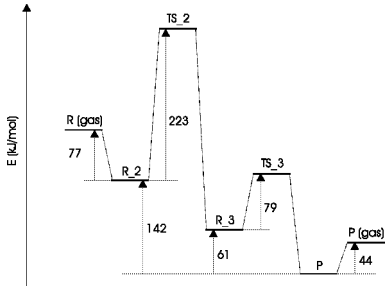

Figure 18. Reaction energy diagram for Beckmann rearrangement catalyzed by external silanol groups. For labels see Figures 15−17.

as in the case of a reaction at a silanol nest, the final reaction step is the lactim−lactam conversion in which silanol groups

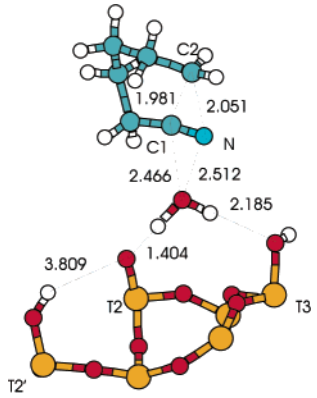

Figure 19. Transition state for the N-insertion catalyzed by isolated silanol group at external surface of mordenite. Selected interatomic distances are in Å.

are not directly involved. The calculated activation energy of 79 kJ/mol is therefore very similar to that for BR at a silanol nest. The structures of the transition state and of the reaction product are shown in Figure17 (TS_3) and (P), respectively. The calculated adsorption energy of ϵ-caprolactam in the final configuration is 44 kJ/mol. The reaction energy diagram is displayed in Figure 18.

Evidently, H-bonding plays a very important role in the stabilization of transition structure for the rate-determining step (N-insertion) of the BR catalyzed by weak BA sites. The H-bonds arranged in the ring, as in the case of silanol nest, allow an efficient stabilization of the siloxy group present in the transition structure for the rate-determining step. The H-bonds of terminal silanol groups stabilize the siloxy group less efficiently and the activation energy increases to 223 kJ/mol. In the absence of any H-bonds, i.e., in the case of isolated silanol groups, the activation energy is even higher. For the rate-determining step of the BR at isolated silanol group T2 (see Figure 5), we calculated a barrier of 266 kJ/mol; the corresponding transition structure is shown in Figure 19.

VII. Calculation of Reaction Rates, Comparison of Reaction Scenarios

To complete the analysis, we have used harmonic transition-state theory to calculate the reaction rates for the BR catalyzed by BA sites and by a silanol nest. The reaction rates are calculated for temperature 623 K, the results are summarized in Table 1, listing the activation energies and reaction rates for all steps of the BR and of the corresponding reverse reactions.

The slowest step for a reaction at a BA site is the R_1 → R_2 transformation ($k_{R\_1\rightarrow R\_2} = 2.71 \times 10^6$ s^{-1}). This reaction step is further hindered by a very fast back-reaction ($k_{R\_2\rightarrow R\_1} = 1.37 \times 10^{12}$ s^{-1}), which is even faster than the reaction step R_2 → R_3 ($k_{R\_2\rightarrow R\_3} = 4.89 \times 10^{11}$ s^{-1}). The reverse reaction modes R_3 → R_2 and P → R_3 are at least 5 orders of

TABLE 1: Calculated Zero-Point Energy Corrected Activation Energies and Rate Constants (T = 623 K) for the Beckmann Rearrangement at Brønsted Acid Site (BA) and Silanol Nest

		BA			silanol nest	
		E_{act} (kJ/mol)	k (s^{-1})		E_{act} (kJ/mol)	k (s^{-1})
$k_{R\_1\rightarrow R\_2}$	N-protonated → H-bonded	88	2.71×10^{6}	N-protonated → H-bonded	42	7.74×10^{8}
$k_{R\_2\rightarrow R\_1}$		9	1.37×10^{12}		7	2.53×10^{12}
$k_{R\_2\rightarrow R\_3}$	N-insertion	64	4.89×10^{11}	N-insertion	149	1.07×10^{4}
$k_{R\_3\rightarrow R\_2}$		115	2.22×10^{6}		245	1.24×10^{-4}
$k_{R\_3\rightarrow P}$	hydrolysis of carbiminium ion	40	3.22×10^{9}	lactim−lactam transformation	72	1.96×10^{8}
$k_{P\rightarrow R\_3}$		201	1.27×10^{-2}		159	1.07×10^{1}

magnitude slower than the corresponding forward steps and can be ignored in further analysis. As the escape rates from points R_2 and R_3 are very fast compared to the slowest forward reaction step, their concentrations can be considered to be negligible compared to concentrations of R_1 in the beginning or of P at the end of the reaction, i.e., $c_{R\_1} + c_P \gg c_{R\_2} + c_{R\_3}$. Hence BR catalyzed by BA sites is effectively an elementary first-order reaction R_1 → P, i.e., the time evaluation of concentration of product can be written as

$$c_P = c^0_{R\_1}(1 - e^{-k_{eff}t}) \tag{2}$$

where $c^0_{R\_1}$ is the initial concentration of reactant R_1 and k_{eff} is an effective reaction rate. It can be shown that for this reaction k_{eff} can be expressed as

$$k_{eff} = \frac{k_{R\_1 \to R\_2} k_{R\_2 \to R\_3}}{k_{R\_1 \to R\_2} + k_{R\_2 \to R\_1} + k_{R\_2 \to R\_3}} \tag{3}$$

Taking into account that $k_{R\_2 \to R\_1}$ is the largest term in the denominator in eq 3, the effective activation energy can be approximated by

$$E^{eff}_{act} \approx E^{R\_1 \to R\_2}_{act} + E^{R\_2 \to R\_3}_{act} - E^{R\_2 \to R\_1}_{act} \tag{4}$$

This is the justification for the very intuitive assumption that the effective activation energy is an energy difference between the highest saddle point (TS_2) and the reactant R_1. For reaction catalyzed by the Brønsted acid site, this combined activation energy is 142 kJ/mol (to be compared with the activation energy of 178 kJ/mol for the rate-determining step (1,2-H shift) in the gas-phase without catalyst); the effective rate constant is 7.13×10^5 s^{-1}.

Similar considerations apply for the BR catalyzed by a silanol nest. In this case the slowest forward reaction is the N-insertion. Again the transformation from an N-protonated to an H-bonded species is an endothermic reaction so that the rate for the reverse reaction ($k_{R\_2 \to R\_1} = 2.53 \times 10^{12}$ s^{-1}) is higher than for the forward reaction ($k_{R\_1 \to R\_2} = 7.74 \times 10^8$ s^{-1}). The effective barrier and the overall rate constant calculated using eq 3 and 4 are 184 kJ/mol and 3.27 s^{-1}, respectively. The reaction catalyzed by silanol nest is thus 5 orders of magnitude slower than that at BA sites.

VIII. Conclusions

The Beckmann rearrangement of cyclohexanone oxime to ϵ-caprolactam catalyzed in mordenite has been studied using periodic ab initio DFT calculations. The active sites considered in this study are a Brønsted acid site, a silanol nest, and H-bonded and isolated terminal silanol groups.

Among the investigated reaction scenarios, the reaction at the BA site has been found to be most favorable for the Beckmann rearrangement. We have shown that this reaction behaves like an elementary first-order reaction of the form R → P with "effective" activation energy of ∼142 kJ/mol. This value is much lower than that estimated for the reaction at weak acid sites (E^{eff}_{act} >184 kJ/mol). From our analysis of reaction rates it follows that a reaction at BA sites is 5 orders of magnitude faster than the reaction at a weak acid site represented by a silanol nest. Moreover, the adsorption energies of cyclohexanone oxime at weak acid sites are much lower than the effective activation energies; the frequent desorption of reactant can cause further retardation of reaction. Although several authors claimed that the strong BA sites are catalytically active in BR,[15,16] it is now generally accepted that an increasing (Al/Si) ratio (and hence an increasing concentration of BA sites) has a negative effect on the conversion rate and the selectivity of the Beckmann rearrangement.[6,58] This is possibly related to the rather high adsorption energy for the ϵ-caprolactam at a BA site. At a high concentration of acid-sites, the product of the BR will be multiply readsorbed and desorbed during diffusion out of the zeolite, and this necessarily reduces the turnover quite substantially. This hypothesis is also supported by the kinetic study of Komastu et al.[10] who found that desorption of ϵ-caprolactam is the slowest reaction process in BR at zeolites. One could also speculate that selectivity rather than reaction rate is the decisive factor in this reaction and that the strong BA sites are more prone to the formation of the byproducts,[6,58,59] but such considerations are out of the scope of the present work.

Hydrogen bonding between OH groups plays a key role in the reaction catalyzed by silanol groups. In a defect forming a silanol nest, four OH groups are H-bonded in such a way that every O atom is donor as well as acceptor of a H atom. This structure allows a rearrangement of the positions of H atoms and in turn a very efficient stabilization of the siloxy group formed during the N-insertion, which is the rate-controlling reaction step. The calculated activation energy for N-insertion is 149 kJ/mol. Such rearrangement is not possible for H-bonded silanol pairs at the external surface of zeolite. Hence the corresponding reaction barrier of 224 kJ/mol is significantly higher than that calculated for a silanol nest. In the absence of H-bonding among silanol groups, the reaction barrier even increases to 266 kJ/mol. Our results suggest that the activity of weak acid sites in the Beckmann rearrangement decreases in the order silanol nest > H-bonded terminal silanol groups > isolated silanol group. This result is in good agreement with experiment.[7,60]

Upon adding a polar solvent such as water or methanol, both the conversion and the selectivity of Beckmann rearrangement are improved.[6,10,61] We have found that molecules of the solvent participate actively in the final step of the Beckmann rearrangement catalyzed by weak acid sites, which is the lactim−lactam conversion. Upon involving a molecule of water or methanol, the reaction barrier for the lactim−lactam transformation decreases from ∼90 kJ/mol to only ∼3 kJ/mol.

Acknowledgment. This work has been performed with the Science College "Computational Materials Science", supported by the Austrian Science Funds. L.B. acknowledges financial support from the Institut Français du Pétrole ELF within the Groupement de Recherche Européen (GdR-E) "Dynamique moléculaire quantique appliquée à la catalyse". The use of facilities at Computing Center of Vienna University is kindly acknowledged.

References and Notes

(1) Hölderich, W. F.; Röseler, J.; Heitmann, G.; Liebens, A. T. *Catal. Today* **1997**, *37*, 353.
(2) Dai, L. X.; Koyama, K.; Miyamoto, M.; Tatsumi, T. *Appl. Catal. A* **1999**, *189*, 237.
(3) Sato, H.; Ishii, N.; Hirose, K.; Nakamura, S. In *Proceedings of the 7th IZC*, Kyoto, Japan, 1986; p 755.
(4) Sato, H. *Catal. Rev. Sci. Eng.* **1997**, *39*, 395.
(5) Flego, C.; Dalloro, L. *Microporous Mesoporous Mater.* **2003**, *60*, 263.
(6) Ichihashi, H.; Kitamura, M. *Catal. Today* **2002**, *73*, 23.
(7) Heitmann, G. P.; Dahlhoff, G.; Hölderich, W. F. *J. Catal.* **1999**, *186*, 12.
(8) Röseler, J.; Heitmann, G.; Hölderich, W. F. *Appl. Catal. A* **1996**, *144*, 319.
(9) Heitmann, G. P.; Dahlhoff, G.; Niederer, J. P. M.; Hölderich, W. F. *J. Catal.* **2000**, *194*, 122.

(10) Komatsu, T.; Maeda, T.; Yashima, T. *Microporous Mesoporous Mater.* **2000**, *35*−*36*, 173.
(11) Dai, L. X.; Hayasaka, R.; Iwaki, Y.; Koyano, K. A.; Tatsumi, T. *Chem. Commun.* **1996**, *9*, 1071.
(12) O'Sullivan, P.; Forni, L.; Hodnett, B. K. *Ind. Eng. Chem. Res.* **2001**, *40*, 1471.
(13) Anand, R.; Khomane, R. B.; Rao, B. S.; Kulkarni, B. D. *Catal. Lett.* **2002**, *78*, 189.
(14) Hölderich, W. F.; Heitmann, G. *Catal. Today* **1997**, *38*, 227.
(15) Aucejo, A.; Bruguet, M. C.; Corma, A.; Fornés, V. *Appl. Catal.* **1986**, *22*, 187.
(16) Camblor, M. A.; Corma, A.; García, H.; Semmer-Herlédan, V.; Valencia, S. *J. Catal.* **1998**, *177*, 267.
(17) Nguyen, M. T.; Raspoet, G.; Vanquickenborne, L. G. *J. Am. Chem. Soc.* **1997**, *119*, 2552.
(18) Nguyen, M. T.; Raspoet, G.; Vanquickenborne, L. G. *J. Chem. Soc., Perkin Trans. 2* **1997**, *4*, 821.
(19) Nguyen, M. T.; Raspoet, G.; Vanquickenborne, L. G. *J. Chem. Soc., Perkin Trans. 2* **1995**, 1791.
(20) Nguyen, M. T.; Vanquickenborne, L. G. *J. Chem. Soc., Perkin Trans. 2* **1993**, 1969.
(21) Fois, G. A.; Ricchiardi, G.; Bordiga, S.; Busco, C.; Dalloro, L.; Spanò, G.; Zecchina, A. In *Proceedings of the 13th International Zeolite Conference*, 2001; p 149.
(22) Shinohara, Y.; Shouro, S. M. D.; Nakajima, T. *J. Mol. Struct.* **2000**, *497*, 1.
(23) Ishida, M.; Suzuki, T.; Ichihashi, H.; Shiga, A. *Catal. Today* **2003**, *87*, 187.
(24) Yamaguchi, Y.; Yasutake, N.; Nagaoka, M. *J. Mol. Struct. (THEOCHEM)* **2003**, *639*, 137.
(25) Boero, M.; Ikeshoji, T.; Liew, Ch. Ch.; Terakura, K.; Parrinello, M. *J. Am. Chem. Soc.* **2004**, *126*, 6280.
(26) Kresse, G.; Hafner, J. *Phys. Rev. B* **1993**, *48*, 13115.
(27) Kresse, G.; Hafner, J. *Phys. Rev. B* **1994**, *49*, 14251.
(28) Kresse, G.; Furthmüller, J. *Comput. Mater. Sci.* **1996**, *6*, 15.
(29) Kresse, G.; Furthmüller, J. *Phys. Rev. B* **1996**, *54*, 11196.
(30) Perdew, J. P.; Chewary, J. A.; Vosko, S. H.; Jackson, K. A.; Pedersen, M. R.; Singh, D. J.; Fiolhais, C. *Phys. Rev. B* **1992**, *46*, 6671.
(31) Perdew, J. P.; Wang, Y. *Phys. Rev. B* **1992**, *45*, 13244.
(32) Blöchl, P. E. *Phys. Rev. B* **1994**, *50*, 17953.
(33) Kresse, G.; Joubert, D. *Phys. Rev. B* **1999**, *59*, 1758.
(34) Baker, J.; Kessi, A.; Delley, B. *J. Chem. Phys.* **1996**, *105*, 192.
(35) Kudin, K. K.; Scuseria, G. E.; Schlegel, H. B. *J. Chem. Phys.* **2001**, *114*, 2919.
(36) Andzelm, J.; King-Smith, R. D.; Fitzgerald, G. *Chem. Phys. Lett.* **2001**, *335*, 321.
(37) Bucko, T.; Ángyán, J.; Hafner, J. GADGET−A program for efficient ionic relaxation, unpublished.
(38) Bucko, T.; Thesis, Universität Wien, 2004.
(39) Farkas, Ö.; Schlegel, H. B. *Phys. Chem. Chem. Phys.* **2002**, *4*, 11.
(40) Broyden, C. G. *J. Inst. Math. Appl.* **1970**, *6*, 76.
(41) Fletcher, R. *Comput. J.* **1970**, *13*, 317.
(42) Goldfarb, D. *Math. Comput.* **1970**, *24*, 23.
(43) Shanno, D. F. *Math. Comput.* **1970**, *24*, 647.
(44) Lindh, R.; Bernhardson, A.; Karlström, G.; Malmqvist, P. Å. *Chem. Phys. Lett.* **1995**, *241*, 423.
(45) Henkelman, G.; Jóhannesson, G.; Jónsson, H. *Methods for Finding Saddle Points and Minimum Energy Paths*, *Progress on Theoretical Chemistry and Physics*; Schwartz, S. D., Ed.; Kluwer Academic Publishers: Dordrecht, 2000; p 272.
(46) Powell, M. J. D. In *Nonlinear Programming*; Rosen, J. B., Mangasarian, O. L., Ritter, K., Eds.; Academic Press: New York, 1970.
(47) Powell, M. J. D. *Math. Prog.* **1971**, *1*, 26.
(48) Murtagh, B.; Sargent, R. W. H. *Comput. J.* **1972**, *13*, 185.
(49) Bofill, J. M. *J. Comput. Chem.* **1994**, *15*, 1.
(50) van Santen, R. A.; Niemantsverdriet, H. W. *Chemical Kinetics and Catalysis*; Plenum Press: New York, 1995; p 139.
(51) Kresse, G.; Furthmüller, J.; Hafner, J. *Europhys. Lett.* **1995**, *32*, 729.
(52) Demuth, T.; Rozanska, X.; Benco, L.; Hafner, J.; van Santen, R. A.; Toulhoat, H. *J. Catal.* **2003**, *214*, 68.
(53) Demuth, T.; Hafner, J.; Benco, L.; Toulhoat, H. *J. Phys. Chem. B* **2000**, *104*, 4593.
(54) Bucko, T.; Benco, L.; Demuth, Th.; Hafner, J. *J. Chem. Phys.* **2002**, *117*, 7295.
(55) Stephens, P. J.; Devlin, J. F.; Chabalowski, C. F.; Frisch, M. J. *J. Phys. Chem.* **1994**, *98*, 11623.
(56) Heldt, W. Z. *J. Org. Chem.* **1961**, *26*, 2552.
(57) Zarakhani, N. G. *Russ. Chem. Rev.* **1967**, *36*, 51.
(58) Sato, H.; Ishii, N.; Hirose, K.; Nakamura, S. In *Proceedings of the 7th IZC*; Murakami, Y., Iijama, A., Ward, J. W., Eds.; 1986; p. 755.
(59) Ushikubo, T.; Wada, K. *J. Catal.* **1994**, *148*, 138.
(60) Forni, L.; Fornasari, G.; Lucarelli, C.; Katovic, A.; Trifirò, F.; Perri, C.; Nagy, J. B. *Phys. Chem. Chem. Phys.* **2004**, *6*, 1842.
(61) Ichihashi, H.; Sato, H. *Appl. Catal. A* **2001**, *221*, 359.